Design study for support of thin glass optical elements for x-ray telescopes

Mark D. Freeman*, Paul B. Reid, William N. Davis
Smithsonian Astrophysical Observatory, 60 Garden St., Cambridge, MA USA 02138

ABSTRACT

The next large x-ray astrophysics mission launched will likely include soft x-ray spectroscopy as a primary capability. A requirement to fulfill the science goals of such a mission is a large-area x-ray telescope focusing sufficient x-ray flux to perform high-resolution spectroscopy with reasonable observing times. One approach to manufacturing such a telescope is a Wolter-I optic utilizing thin glass segments rather than full shells of revolution. We describe a parameterized Finite Element Modeling (FEM) study that provides insights useful in optimizing the design of a discrete support system to balance the competing requirements of minimizing the effect on optical performance while providing sufficient support to withstand launch loads. Parameters analyzed are number and location of the supports around the glass segments, as well as the glass thickness, size, and angular span. In addition, we utilize more detailed models of several cases taken from the parametric study to examine stress around the bonded area and bond pad size, and compare the stress from the detailed model to the parametric cases from which they were derived.

Keywords: x-ray optics, mirror support systems, finite element modeling and analysis, parametric study

1. INTRODUCTION

The success of the Chandra X-ray Observatory has led to the need for a large area x-ray spectroscopy mission. Constellation-X (Con-X) is NASA's next priority in large x-ray astronomy missions. The 2000 Decadal Survey confirmed this, assigning Con-X the second highest priority for large missions, behind only the James Webb Space Telescope. Con-X is designed to probe questions surrounding black holes and General Relativity, the origin and evolution of the universe, and further the search for dark energy and matter. Indeed, similar fundamental science goals have been the impetus for the Xeus mission currently under study by the European Space Agency (ESA) as their next major high-energy astrophysics platform. Common to both missions is a soft x-ray telescope with large collecting area and moderate imaging performance.

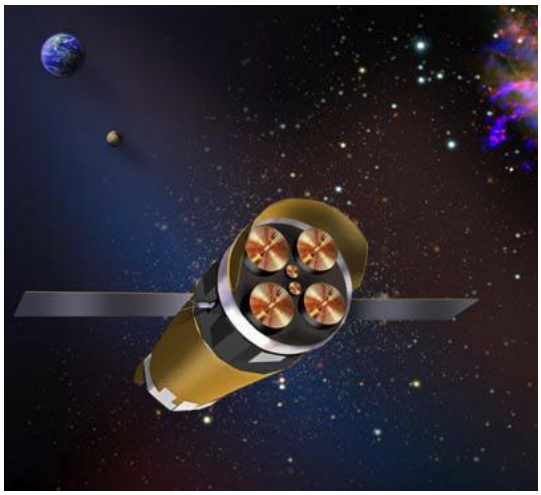

The overall Constellation=X mission is described in references 1 and 2. In its most recent conception, Con-X contains four Spectroscopy X-ray Telescopes (SXTs) with a bandwidth of 0.25 to 12 keV. The four SXTs, utilizing closely nested thin glass elements, are mounted in a single spacecraft and launched on an Atlas 551 and provide a combined effective area that exceeds the fundamental mission requirement of 1.5 m^2 at 1.25 keV and 0.6 m^2 at 6 keV, while maintaining imaging performance of 15 arcsec (5 arcsec goal). To accomplish this, the SXT mirror assemblies are divided into segments, both radially and azimuthally. The current 1.32 diameter SXT design has five 72° azimuthal segments in an inner ring, surrounded by an outer ring of ten 36° segment modules. With primary and secondary mirror modules containing almost 100 thermally formed ("slumped") mirror segments each (see references 3 and 4), a total of 2600 glass segments must be mounted in a single SXT with optical precision whilst supported sufficiently well to withstand the rigors of launch.

* email: mfreeman@cfa.harvard.edu phone: (617)495-7106

Space Telescopes and Instrumentation 2008: Ultraviolet to Gamma Ray, edited by Martin J. L. Turner, Kathryn A. Flanagan, Proc. of SPIE Vol. 7011, 701113, (2008) · 0277-786X/08/$18 · doi: 10.1117/12.787984

This module-based approach to supporting mirror segments must allow for precision alignment while maintaining a common focus for all segments (references 5 and 6), and to do so without disturbing the precision optical design of the individual slumped segments. It can be seen in Figure 1 that the modular structure allows for the possibility of holding the segments either on their ends (axially fore and aft) or along their (azimuthal) edges. Both schemes have been used for various mount concepts and alignment approaches. In this paper we describe a study of mounting the slumped segments with a varying number of discrete points along the segment edges and ends, and with segment sizes spanning the full range contained within this SXT design.

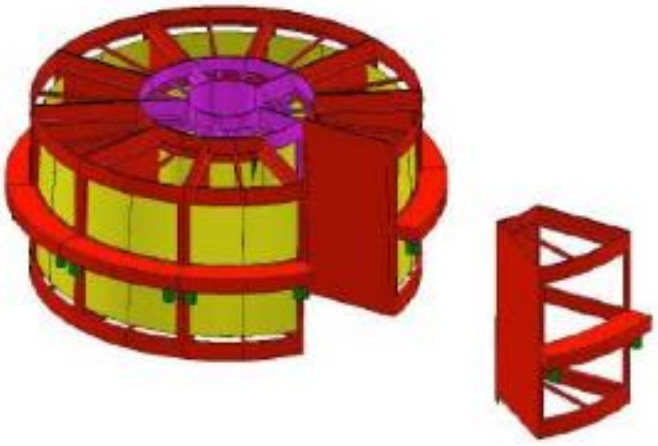

Figure 1. Conceptual SXT telescope assembly, one pair of modules removed

2. PARAMETRIC STRESS STUDY OF MIRROR SEGMENT ATTACHMENT

The Constellation-X mission, despite many configuration variations, has consistently included SXTs with thin glass segments assembled in a modular structure. Although the exact size and angular span of the modules have gone through several iterations, there have been two fundamental guidelines that derive from the slumping process that have limited the module size and span to a manageable range: (1) Limits on forming mandrel size and the slumping process itself have driven the project toward a consistent segment length of approximately 200mm, and (2) The selected glass (Schott D263) is readily available in sheet widths of 400mm. Various assembly schemes have been proposed that hold the glass on ends or edges whose prime motivation has been alignment of the mirror segments, with little consideration given to the relative merit of these schemes from the structural (primarily launch load) standpoint.

We describe a parametric finite-element analysis-based study designed to determine the relative merits of these mounting schemes from the standpoint of mirror integrity, recognizing that certain parametric directions likely result in worsening optical performance, primarily due to over-constraint. However, the desire here is to understand the trends, and whether or not there are clear break-points in them, with the hope of identifying an optimum balance between the structural and optical requirements.

2.1 Study Parameter Space

In the study, we compare holding the mirror segments on "ends" (along the fore and aft edges forming the diameter of the shell) vs. "sides" (which break the shell of revolution into segments). In addition, we vary the following:

- **Number of supports (2 to 6), all clamped in 6 DOF (worst case for peak stress)**
- **2 support types (equally spaced, starting at *corners* or *inboard* at 1/(2*n) points)**
- **3 glass thicknesses (0.2, 0.4, 0.7 mm)**
- **6 radii (3 each inner and outer module – innermost, most central, outermost)**

This parameter space encompasses the majority of the variations considered over the span of the Con-X program, as well as glass thickness, which has been discussed both in the context of better optical performance (thicker) and reducing overall SXT mass (thinner).

A total of 360 distinct FEA models are described by this parameter list; because of the large number, we generated the models in ANSYS™ automatically, using a script. An explicit node/element layout was used around each attachment

point that remained consistent throughout the entire study, to minimize stress results variability due to element size and shape variation in these highest-stress areas. Auto-meshing was used to mesh the remaining mirror area. Figure 2 shows the four fundamental variations of the attachment schemes; the cyan highlights the finely-meshed areas around the bond points. Attachment is to ground in all 6 degrees-of-freedom, simulating and infinitely stiff support frame.

Three load cases were run on each of the 360 models representing a 1g load in each of the three principal axes: Z is the optical axis of the mirror shells, X is radially outward through the center of the segment, and Y completes the triad (tangential at the mirror center). Results were tabulated for both the maximum principal stress and the maximum principal stress outside the finely meshed areas near the supports; the latter was used to provide a means of determining whether or not trends seen in the peak stress held throughout the larger mirror area.

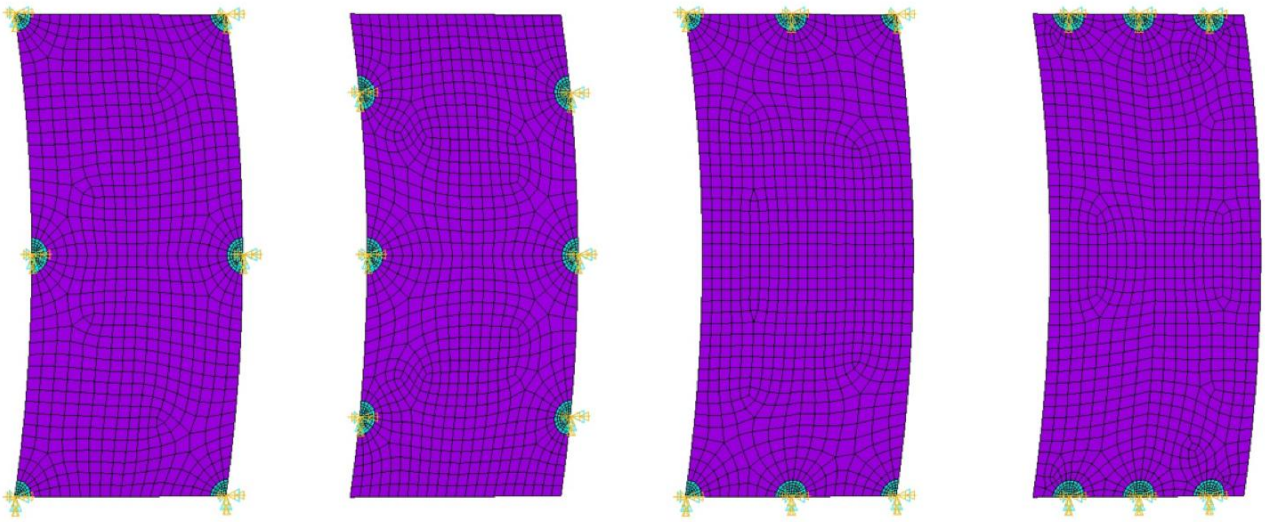

Figure 2. Representative examples of the 4 fundamental mirror attachment schemes studied: (a) Ends to corners, (b) Ends inboard, (c) Sides to corners, and (d) Sides inboard. Illustrated cases are a 36° segment shown with the optical axis approximately horizontal

2.2 Initial Study Results and Observations

The large number of data points required many iterations of data presentation to create an understandable display of the trends. We ultimately settled on a basic format, consisting of all six segment sizes (outermost to innermost) displayed in six panels with a common ordinate axis of maximum stress. Within each panel, the abscissa is the number of support points (2 to 6) from left to right. A sample of this display of results is shown in Figure 3, representing the maximum principal stress for 0.4mm thick (nominal) mirrors for 15g X and Z loads [results were initially scaled to 15g to represent a reasonable estimate of launch loads]. A full set of results (all thicknesses and load directions) is available on request.

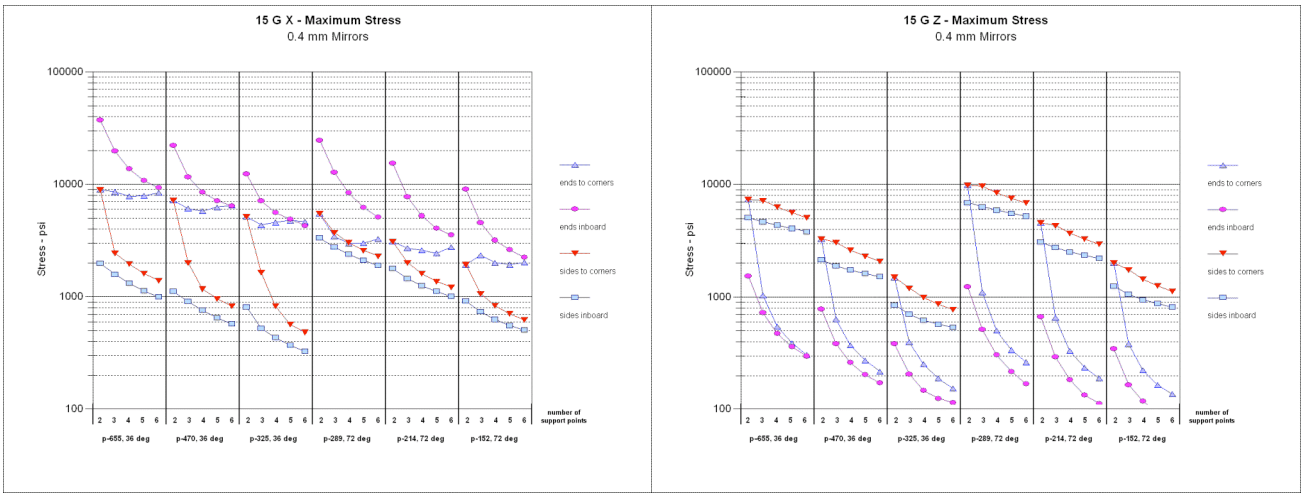

Figure 3. Maximum principal stress (psi) for 15g X load (radially outward on segment, left plot) and 15g Z load (along optical axis, right plot) for 0.4mm thick mirror segments. Each of the 6 panels within a plot represents a segment size (outermost to innermost) with varying number of supports (2 to 6).

An alternative scheme for displaying the results is shown in the example plots in Figure 4, where the results for a particular support configuration (e.g. Ends to corners) are shown in each plot, and the three curves represent the three load directions. This is useful in assessing load direction that produces the maximum glass stress.

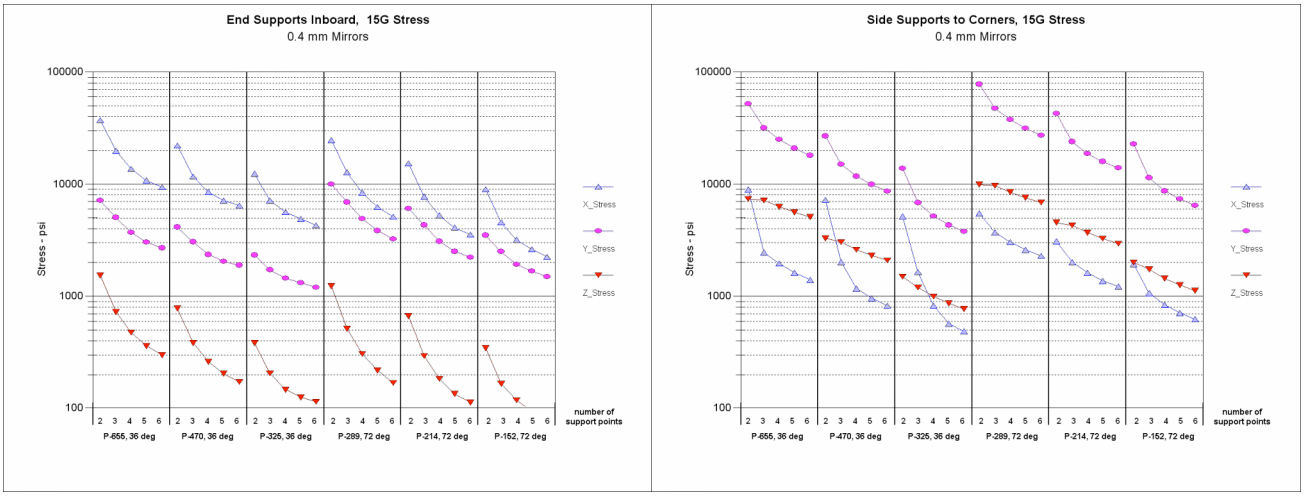

Figure 4. Maximum principal stress for the 3 load directions for a particular support configuration. Shown are End Supports Inboard (left) and Side Supports to Corners (right).

Several fundamental observations were made in examining the full set of plots of these results. Although not shown in the plotted results herein, stress scaled at approximately 1/thickness, the expected result from thin shell theory, and provides useful information for scaling should we be driven to another thickness. However, for the remainder of the paper we will focus on results for the current nominal thickness of 0.4mm.

It can be seen in the results that the calculated principal stress for the different load cases and support configurations varies by almost three orders of magnitude. An expected result is that in all cases, increasing the number of supports decreased the maximum stress; not obvious *a priori*, however, was the frequent sharp drop in stress from 2 to 3 supports per edge, and then a general flattening as the number of supports increased from 3 to 6, particularly in the X and Y load direction cases. A fundamental principle lies behind this behavior: The supported edges "force" a basic first mode shape; increasing the number of supports along the same edge does not alter this but rather adds stiffness incrementally to the supported edge. Additionally, in most cases the X and Y load directions produced the largest stresses. This is

principally due to the stiffness of the segment resulting from its curvature, coupled with the relative distance from the support points to the mirror segment's center of mass (perpendicular to the load direction).

The preceding plots still fall short in assessing all cases simultaneously. In those of the form of Figure 3, the different configurations can easily be compared for a given load direction but make it difficult to compare the configurations for a more complicated load case, such as 3-axis random vibration. Conversely, the representations in Figure 4 are useful in giving a complete picture of a single configuration of supports, but do not allow easy comparison of the configurations. As an alternative that allows the full set of results to be displayed in a single plot, we combine the three load directions in a way that represents a reasonable analog of the load case of interest: launch. The Z axis is the presumed launch direction, which generally produces the highest loads. Since the segments are distributed around the diameter of the SXT symmetrically, X and Y loads must be combined at the same magnitude (for every segment experiencing an X-directed load, there is an identical segment 90° away experiencing a Y load of the same magnitude. Based on experience with several telescope programs' launch requirements, we settled on a "combined" stress consisting of the root-sum-square (RSS) of a 15g Z load and 7.5g loads in X and Y. In Figure 5, we plot the combined tri-axial stress for the four configurations. As mentioned above, we also tabulated stress for the mirror area exclusive of the area immediately surrounding the bond pad; this plot is included on the right side of the figure for comparison.

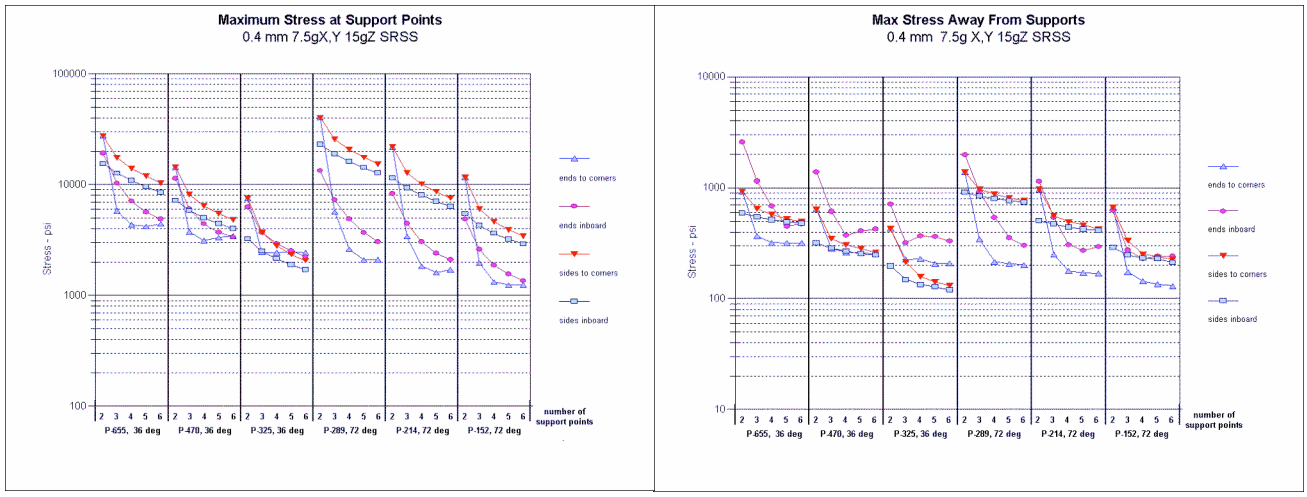

Figure 5. Combined 3-axis loads ($\sqrt{15Z^2 + 7.5gX^2 + 7.5gY^2}$) for all four support configurations. Left plot is maximum principal stress; right is maximum principal stress away from the support points.

The fully combined results yield some useful additional insights. Comparing the entire set of 6 mirror radii (the full range of this SXT configuration, the end support cases yield the lowest stress if we discount the 2 support point cases, where the stress is universally too high. Additionally, little improvement obtains from increasing the number of supports beyond four for these cases. It is also clear that for the side support cases, the high stresses are not significantly reduced by adding support points, particularly for the inner (72°) shells.

The results of this portion of the study are useful in understanding the differences in the support configurations and the trends in the stress picture with varying parameters. The simplicity of the model, however, suggests these results be used only to judge relative performance; the simple supports and use of shell elements in the model cannot be considered to yield reliable estimates of the absolute stress. In the next section, we study three individual cases encompassed by this work in sufficient detail to do so and provide useful scaling information for these results.

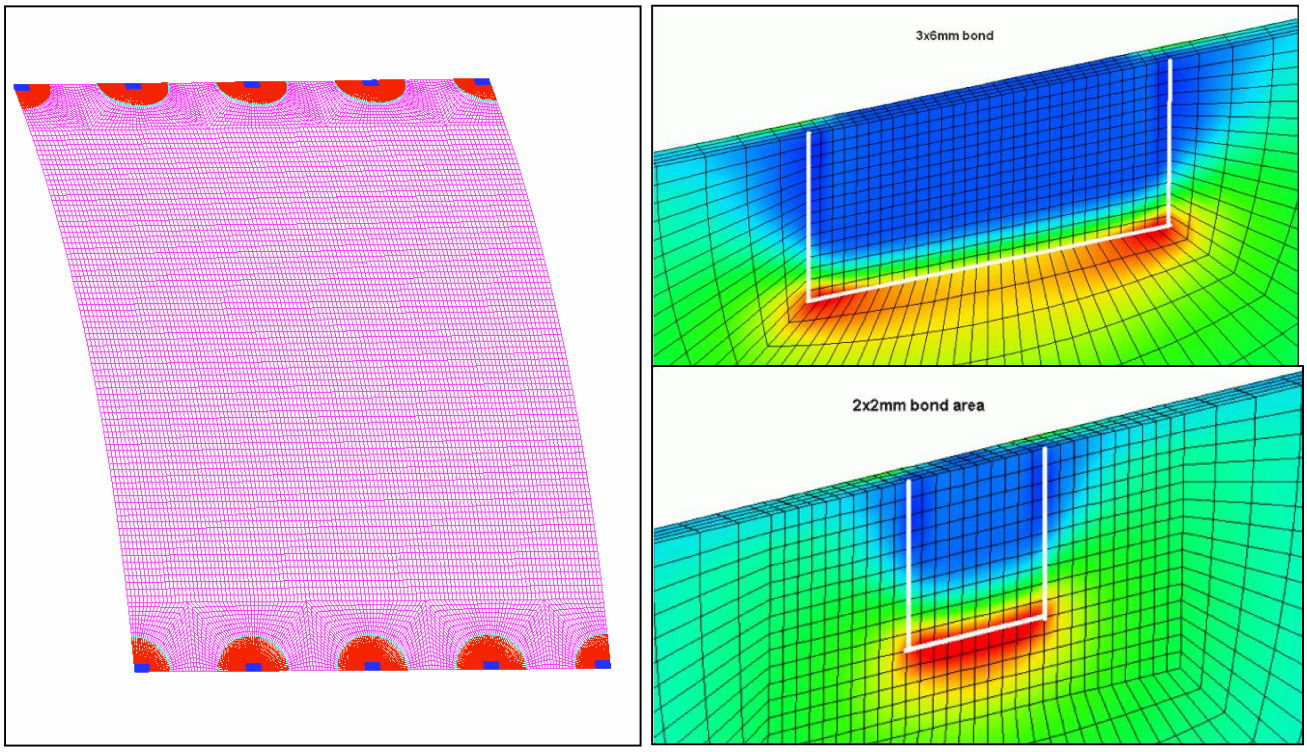

Figure 6. FEA Detailed Model Example: Left box shows the element layout for the 5 attachment (sides to corners) model. Red areas are modeled with 4 solid elements through the glass thickness, with the remainder (cyan) shell elements. Right hand boxes are details of the glass portion of the bond pad area with a sample stress distribution; upper box is the largest (3 x 6 mm) bond area, and the lower box is the smallest (2 x 2 mm) bond area (both outlined in white).

3. DETAILED ANALYSIS OF THREE CASES

The study of the previous section utilized a simple FEA model design to allow a large number of models to be created in an automated way due to the large number of distinct models. In this section, we have taken three specific cases derived from specific SXT configurations that have been proposed. The two fundamental cases are: (1) The segment held at 5 points on the ends (inboard) and (2) The segment is held at 3 points along the edges, ends and in the middle (corners). We then selected a third case (5 edge supports to corners) to provide a "bridge" case, to help separate the effects of more supports from those related to the configuration itself.

The model for this portion of the study requires a high level of detail in the bond pad area to minimize the effects of joint discontinuities (Figure 6). We modeled the glass with four elements through the thickness, and then an epoxy layer of one element thickness on either side of the glass. The other side of the epoxy layer was attached to rigid ground, as in the parametric portion of the study. We explored some additional parameter space in the epoxy joint: Bond pad size (3 x 6 mm to 2 by 2 mm), thickness of the epoxy layer (0.002 in. to 0.012 in.), and modulus of elasticity of the epoxy (250 ksi to 750 ksi).

3.1 Epoxy Stress in the Bond

The detailed model provides insight into the epoxy behavior in the bonds as well as the glass. Although not the focus of this work, we compiled figures for the maximum stress in the epoxy with variations in the modulus, bond thickness, and size of the bond pad. Overall, the stress was within a reasonable range for epoxies; the variation resulting from exercising the parameters for this section of the study yielded the following conclusions:

- **The epoxy stress was not a significant function of the epoxy *thickness***
- **The epoxy stress increases with increasing epoxy Young's modulus (by approximately $E^{0.56}$)**

- **The epoxy stress increases with fewer bond points and/or less bond area (similar to glass stress)**

The second bullet is the only one that might not follow one's intuition. Inspection of the detailed stress distribution shows that the higher modulus concentrates the stress in a smaller area (near the corners of the bond area) and since we are tabulating the maximum principal stress, the result is higher.

3.2 Stress in the Glass

Understanding the stress in the glass for these configurations is the principal goal of these analyses. The results provide a very good picture of the particular configurations studied, but also provide a sense of the scale factor between the results of the previous parametric study (shown as "coarse model" in **Error! Reference source not found.**) and a more detailed analysis.

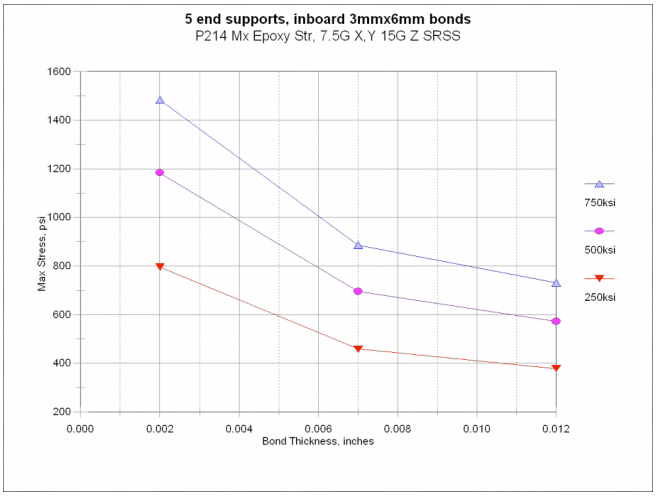

Figure 7. Epoxy stress as a function of modulus and thickness

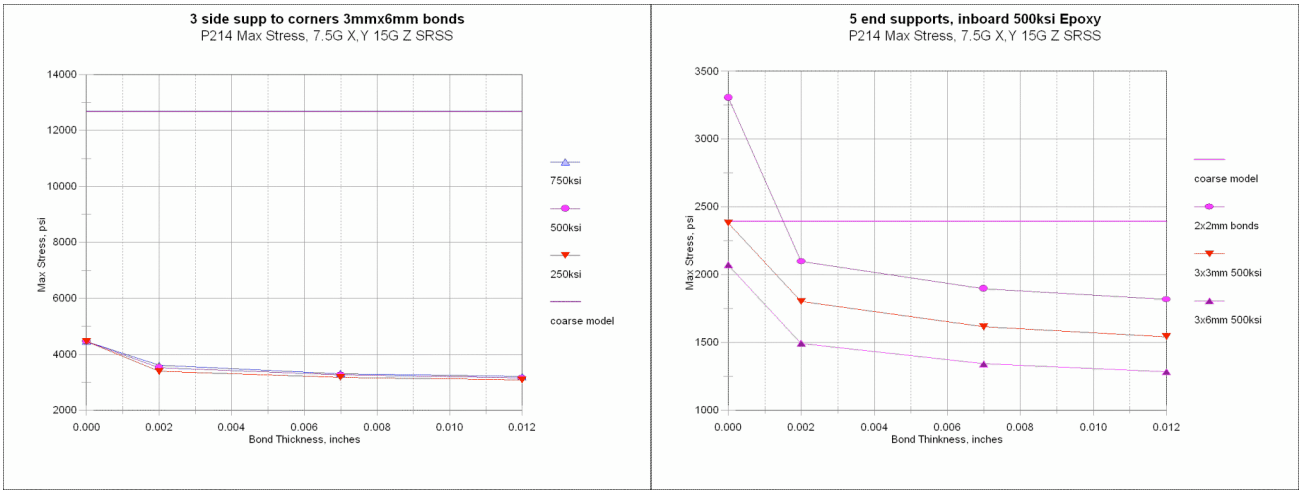

Figure 8. Glass stress for the two fundamental cases in the detailed study. The left plot shows the absence of a dependence of the glass stress on both epoxy modulus and bond thickness, and shows that for this case the detailed model yields a stress approximately 1/3 that of the coarse model. The right plot shows results for the 5 end supports (inboard) and the dependence on bond pad size.

In the left plot in Figure 8, we the results for the 3 bonds per side (to ends) configuration as a function of the bond thickness and epoxy modulus, showing the glass stress almost no dependence on either parameter, a result repeated for all of the cases. [Note that in the plots in this section, the leftmost point (Bond Thickness = 0.0), we have plotted the results for a rigid attachment to ground.] The line near the top of the plot area is the result for this case in the earlier parametric study; we find that in this case, the detailed model yields stresses approximately ¼ that of the earlier work. The right plot of this figure is the result for the 5 bonds on the ends (inboard) and shows the typical dependence on bond pad size. In this case the stress in the detailed model is more ½ that of the coarse model. We note a general trend toward closer agreement between the coarse and detailed results as the number of attachment points increases.

Summarizing the results:

- **Maximum principal stress in the *glass segments* is not a significant function of either epoxy modulus or bond thickness.**

- **Glass stress is strongly dependent on the number of attachments points and the area of the bond pad (e.g. the stress for the 3 pad configuration (left in** Error! Reference source not found.**) is approximately 3100 psi; the stress for the 5 pad configuration in the right plot is ~1300 psi for the same bond pad design).**

To this point, we have not discussed a failure criterion for the glass segments, although clearly that is the ultimate goal of this work. There are several factors to keep in mind when considering this: (1) The failure mechanism is brittle fracture, requiring a high factor of safety in any launch failure analysis, (2) Brittle fracture is a statistical process, generally following a Weibull distribution, and (3) The small bond pads (relative the the glass segment size) result in a very small area of high stress; for most of the glass area, the glass stress is more than 2 orders of magnitude less than the maximum. Bearing this in mind, and given the ultimate strength of this particular glass is approximately 8 ksi, and further assuming that the required factor of safety for brittle materials will be 5, we believe that the stress for at least the cases with 4 supports per edge are robust enough for this support type to be viable, although further analysis using Weibull statistics and the effect of stressed area is needed.

4. CONCLUSIONS AND PLANNED FUTURE WORK

We have undertaken a study of the glass stress for closely packed thin glass segments supported symmetrically by a discrete number of small bond pads. In the first section, we studied the maximum stress while varying parameters related to the overall configuration of the supports, particularly number and location on the segment perimeter, and the direction of the applied load. We conclude that more than 4 support points (2 per side) are needed, and that there is little additional benefit beyond 4 supports per side in any configuration. We also conclude that for the nominal launch configuration, end supports yield slightly better performance than side supports.

In the second section we examined three configurations in more detail, since the simple model of the preceding study was not sufficiently detailed to estimate the absolute glass stress (although useful as a relative measure against other configurations). Using a model with great detail in the bond area and a representation of the epoxy, we showed that the simple model overestimates the peak stress by a factor of 2 to 4, but the behavior of the results followed the same trends. In addition, both the epoxy stress and the glass stress are low enough to establish viability for this type of support system for the glass segments, and that the glass stress is not significantly affected by the epoxy or the details of the joint thickness. It is, however, strongly dependent on both the size bond pad and the number of supports.

Several additional factors should be considered in any application of the stress results presented herein. First, this study presented only the results of self-loading from the glass segment mass; the support system was assumed to be infinitely rigid. In a real telescope assembly, the flexibility of the support structure and the interaction between the stiffness of the many glass segments in a module and the structure will have to be analyzed. Second, this study does not consider the effects of acoustic loading. Typically, some fraction of the total allowable loads must be partitioned to acoustics; in this case, with thin segments of a large surface area, acoustic loads could be important. Lastly, the large number of glass segments, coupled with their brittle nature, will necessarily drive any strength analysis and optimization into employing a Weibull statistical analysis of the failure probability.

In follow-on work, we plan to design a quasi-static test to simulate the load conditions shown in this study, and compile statistics on the failures. We will compare the results to the assumed Weibull distribution, and perform comparison to other failure studies employing this and similar glass elements. In particular, we plan to correlate these studies making appropriate adjustment for the stressed area of the support in this particular configuration.

REFERENCES

[1] N.E. White and H. Tananbaum, "Constellation-X Mission: Science Objectives and implementation Plan", SPIE Proc., vol. **4851**, 293 (2003).

[2] R. Petre, *et al.*, "Constellation-X Spectroscopy X-ray Telescope (SXT)", SPIE Proc., vol. **4851**, 433 (2003).

[3] R. Petre, *et al.*, "Status of the Constellation-X Mission", SPIE Proc., vol. **6686**, .

[4] William Zhang, David Content, Stephen Henderson, John Lehan, Robert Petre, Timo Saha, Stephen O'Dell, William Jones, William Podgorski, and Paul Reid, "Development of Lightweight X-Ray Mirrors for the Constellation-X Mission", SPIE Proc. **5488**, 820 (2004).

[5] Paul B. Reid, *et al.*, "A comparison of different alignment approaches for the segmented grazing incidence mirrors on Constellation-X," SPIE Proc., *to be published these proceedings*.
[6] William Podgorski, David Caldwell, William Davis, Mark Freeman, Scott Owens, Paul Reid, and William Zhang, "A mounting and alignment approach for Constellation-X mirror segments," SPIE Proc., *to be published these proceedings*.